Cell

The Mechanism of Linkage-Specific Ubiquitin Chain Elongation by a Single-Subunit E2

Katherine E. Wickliffe,[1,5] Sonja Lorenz,[1,5,*] David E. Wemmer,[1,2,4] John Kuriyan,[1,2,3,4] and Michael Rape[1,*]
[1]Department of Molecular and Cell Biology
[2]Department of Chemistry
[3]Howard Hughes Medical Institute
University of California, Berkeley, CA 94720, USA
[4]Physical Biosciences Division, Lawrence Berkeley National Laboratory, Berkeley, CA 94720, USA
[5]These authors contributed equally to this work
*Correspondence: slorenz@berkeley.edu (S.L.), mrape@berkeley.edu (M.R.)
DOI 10.1016/j.cell.2011.01.035

SUMMARY

Ubiquitin chains of different topologies trigger distinct functional consequences, including protein degradation and reorganization of complexes. The assembly of most ubiquitin chains is promoted by E2s, yet how these enzymes achieve linkage specificity is poorly understood. We have discovered that the K11-specific Ube2S orients the donor ubiquitin through an essential noncovalent interaction that occurs in addition to the thioester bond at the E2 active site. The E2-donor ubiquitin complex transiently recognizes the acceptor ubiquitin, primarily through electrostatic interactions. The recognition of the acceptor ubiquitin surface around Lys11, but not around other lysines, generates a catalytically competent active site, which is composed of residues of both Ube2S and ubiquitin. Our studies suggest that monomeric E2s promote linkage-specific ubiquitin chain formation through substrate-assisted catalysis.

INTRODUCTION

By regulating protein stability, activity, or localization, ubiquitination exerts control over almost every cellular process. As this includes pathways responsible for the duplication and separation of genetic material, aberrant ubiquitination often results in tumorigenesis. Despite the importance for cellular regulation, the mechanisms determining the specificity and efficiency of ubiquitination reactions are still incompletely understood.

Ubiquitination requires at least three enzymatic activities. An E1 enzyme forms a thioester between a cysteine at its active site and the C terminus of ubiquitin (Schulman and Harper, 2009). The activated ubiquitin is transferred to a cysteine of an E2 (Ye and Rape, 2009). In the third step, the charged E2 cooperates with E3s to catalyze formation of an isopeptide bond between the C terminus of ubiquitin and the ε-amino group of a substrate lysine (Deshaies and Joazeiro, 2009). The ~600 human RING-E3s interact with E2s and substrates at the same time, allowing them to promote the transfer of ubiquitin directly from the E2 to the substrate.

The modification of a substrate with a single ubiquitin usually leads to changes in protein interactions (Dikic et al., 2009). In many cases, additional ubiquitin molecules are attached to a substrate-linked ubiquitin, giving rise to polymeric ubiquitin chains. Such chains can be connected through the N terminus of ubiquitin or through one of its seven Lys residues, and all linkages have been detected in cells (Ye and Rape, 2009; Xu et al., 2009). Ubiquitin chains of different topologies can have distinct structures and functions (Dikic et al., 2009; Matsumoto et al., 2010). K48-linked chains, for example, drive protein degradation, whereas K63-linked chains regulate the assembly of protein complexes (Ye and Rape, 2009). Thus, the efficiency and specificity of chain formation have profound consequences for the modified protein.

We recently identified K11-linked ubiquitin chains as critical cell-cycle regulators in human cells (Jin et al., 2008). Most K11-linked chains are synthesized during mitosis by the E3 anaphase-promoting complex (APC/C) and its E2s Ube2C/UbcH10 and Ube2S (Williamson et al., 2009; Matsumoto et al., 2010; Wu et al., 2010). Together, these enzymes modify mitotic regulators, such as cyclin B, securin, or HURP, to trigger their degradation (Jin et al., 2008; Song and Rape, 2010). As a result, inhibiting the formation of K11-linked chains blocks mitotic progression in *Xenopus*, *Drosophila*, and humans (Jin et al., 2008; Williamson et al., 2009; Garnett et al., 2009), whereas their untimely assembly causes inaccurate cell division and tumorigenesis (Wagner et al., 2004; Jung et al., 2006). How the APC/C and its E2s assemble K11-linked chains, however, is poorly understood.

Linkage between two ubiquitin moieties involves the covalent connection of one ubiquitin, the donor, to the active site cysteine of the E2, followed by nucleophilic attack by a lysine of an acceptor ubiquitin (Figure 1A). Much of our knowledge about the basis of linkage specificity is limited to the E2

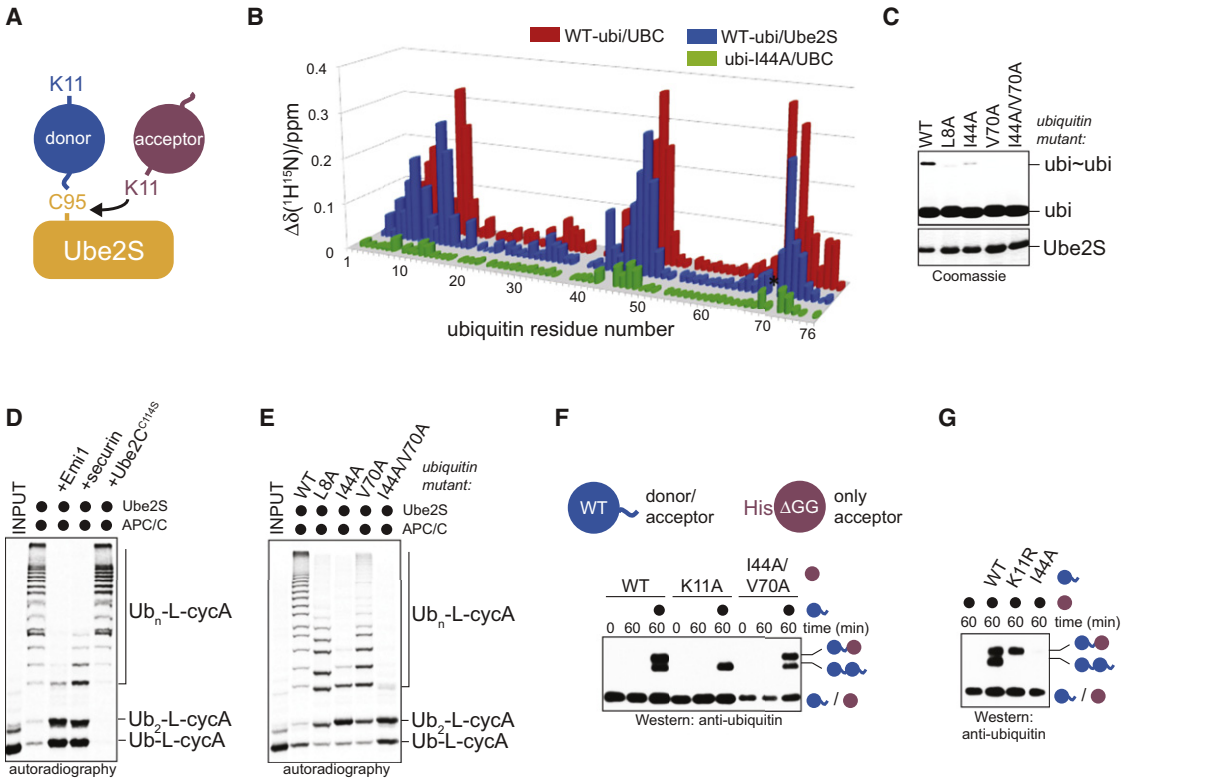

Figure 1. Ube2S Recognizes the Hydrophobic Patch of Donor Ubiquitin

(A) Overview of K11-specific linkage formation. Lys11 of acceptor ubiquitin attacks the thioester bond between Cys95 of Ube2S and the C terminus of the donor ubiquitin.

(B) Ube2S interacts with ubiquitin noncovalently. Weighted combined chemical shift perturbations, $\Delta\delta(^{1}H^{15}N)$, are plotted over residue number. The asterisk indicates the disappearance of the resonance for His68 of ubiquitin in the presence of Ube2S due to intermediate exchange.

(C) Mutation of the hydrophobic patch in ubiquitin interferes with formation of K11-linked ubiquitin dimers (ubi~ubi) by Ube2S, as monitored by Coomassie staining.

(D) Ube2S and APC/C extend ubiquitin chains on a fusion between ubiquitin and cyclin A (Ub-L-cycA), as analyzed by autoradiography.

(E) The hydrophobic patch of ubiquitin is required for chain elongation by APC/C^{Cdh1} and Ube2S, as analyzed by autoradiography.

(F) The hydrophobic patch is not required on acceptor ubiquitin. Ube2S was mixed with acceptor ^{His6}ubiquitin$^{\Delta GG}$ mutants (ubi$^{\Delta GG}$; purple) and WT-ubiquitin (blue) and analyzed by α-ubiquitin-western.

(G) The hydrophobic patch is required on the donor ubiquitin. Ube2S was mixed with WT-ubi$^{\Delta GG}$ and ubiquitin mutants and analyzed by α-ubiquitin-western.

See also Figure S1.

Ube2N-Uev1A (Ubc13-Mms2; VanDemark et al., 2001). In this system, the catalytically inactive Uev1A orients the *acceptor* ubiquitin, such that Lys63 of the acceptor is at the active site of Ube2N charged with the donor (Eddins et al., 2006). In contrast, K11- and K48-linkage-specific E2s promote chain elongation in reconstituted systems lacking UEVs (Li et al., 2009; Pierce et al., 2009; Williamson et al., 2009). Although kinetic analyses suggest that these E2s also engage acceptor ubiquitin residues (Petroski and Deshaies, 2005; Rodrigo-Brenni et al., 2010), the molecular details of acceptor recognition by monomeric E2s and its importance for linkage-specific chain formation have not been established.

Here, we have combined functional studies with nuclear magnetic resonance (NMR) and computational docking to dissect the mechanism of linkage-specific chain formation by single-subunit E2s. We show that the K11-specific Ube2S orients the *donor* ubiquitin by a noncovalent interaction that is in addition to the flexible covalent linkage between these molecules at the E2 active site. We find that a similar tethering mechanism is used by other E2s independently of linkage specificity. The Ube2S-donor ubiquitin complex transiently engages the acceptor ubiquitin through electrostatic interactions. As indicated by our analysis, only binding of the acceptor surface around Lys11, but not around other lysines, leads to formation of a catalytically competent active site composed of residues of both Ube2S and ubiquitin. Hence, linkage-specific ubiquitin chain formation by Ube2S is the result of substrate-assisted catalysis.

RESULTS

A Noncovalent Interaction with Ubiquitin Is Required for Ube2S Activity

In the absence of the APC/C, Ube2S generates K11-linked ubiquitin dimers (ubi_2) and chains attached to Lys residues of its UBC

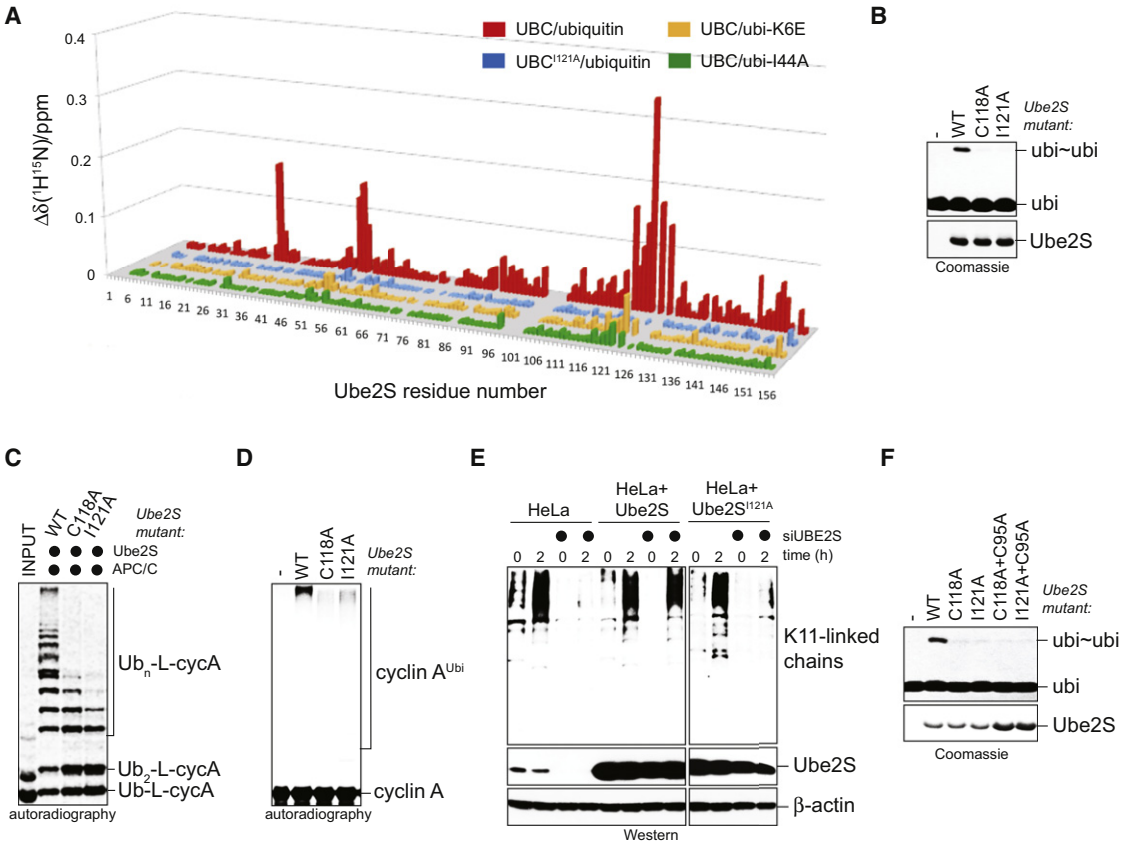

Figure 2. Noncovalent Donor Ubiquitin Binding Is Required for Ube2S Activity

(A) Identification of Ube2S residues involved in noncovalent binding of ubiquitin. Weighted combined chemical shift perturbations, $\Delta\delta(^1H^{15}N)$, are plotted over the residue number.

(B) Donor binding is required for formation of ubi_2 dimers (ubi~ubi) by Ube2S mutants, as analyzed by Coomassie staining.

(C) Donor binding by Ube2S is required for chain elongation on Ub-L-cycA with APC/C, as analyzed by autoradiography.

(D) Donor binding by Ube2S is required for chain formation in a full APC/C assay. Ubiquitination of cyclin A by APC/C, Ube2C, and Ube2S mutants was analyzed by autoradiography.

(E) Donor binding is required for Ube2S activity in vivo. HeLa cell lines expressing Ube2S or $Ube2S^{I121A}$ were treated with siRNAs against the 3′ UTR of Ube2S, which specifically depletes endogenous Ube2S. Cells were synchronized in prometaphase (t = 0 hr) or late mitosis (t = 2 hr), and K11-linked ubiquitin chains were detected by αK11-western.

(F) Donor binding occurs in *cis*. $Ube2S^{C118A}$ or $Ube2S^{I121A}$ (lack the noncovalent ubiquitin-binding site) and $Ube2S^{C95A}$ (no active site) were mixed, and ubi_2 formation was monitored by Coomassie staining.

See also Figure S2.

domain and its C-terminal tail (Figure S1A available online). The UBC domain of Ube2S (UBC^{Ube2S}) promotes ubi_2 formation with similar kinetics and specificity as Ube2S (Figure S1A). Like Ube2S, UBC^{Ube2S} is monomeric in ubiquitination buffers, as suggested by gel filtration, small-angle x-ray scattering (SAXS), and other biophysical techniques (Figures S1B and S1C; data not shown). Thus, UBC^{Ube2S} contains all elements required for the synthesis of K11 linkages, making it an appropriate system for analyzing the mechanism of linkage-specific chain formation.

The prevailing model of linkage-specific chain formation posits that an elongating E2, charged with the donor ubiquitin, binds the acceptor in such a way that a preferred acceptor lysine is at the E2 active site (Eddins et al., 2006). To test for such a noncovalent interaction between Ube2S and ubiquitin, we performed titrations of ^{15}N-enriched ubiquitin with Ube2S and UBC^{Ube2S}, respectively, and monitored ^1H-^{15}N HSQC spectra. The presence of either E2 caused significant resonance-specific chemical shift perturbations in the ubiquitin spectrum, indicating a specific interaction (Figure 1B).

Chemical shift mapping on the surface of ubiquitin revealed that the hydrophobic patch surrounding Ile44 is involved in the noncovalent interaction with Ube2S (Figure S2B). Mutation of the isoleucine to alanine (ubi^{I44A}) disrupted the interaction with Ube2S (Figure 1B and Figure 2A). Furthermore, mutating residues in the hydrophobic patch (L8A, I44A, V70A) interfered strongly with the formation of K11-linked ubi_2 by Ube2S (Figure 1C).

Ube2S extends K11-linked chains on APC/C substrates after initiation by Ube2C (Williamson et al., 2009; Wu et al., 2010). To test whether mutations in ubiquitin interfere with chain elongation

by Ube2S and APC/C, we bypassed the need for Ube2C by generating a fusion between ubiquitin and the APC/C substrate cyclin A (Ub-L-cycA). Ube2S and APC/C rapidly elongated ubiquitin chains on Ub-L-cycA, which did not require Ube2C and was not inhibited by an excess of inactive Ube2C^{C114S} (Figure 1D). Mutation of the hydrophobic patch of ubiquitin interfered strongly with this activity of Ube2S (Figure 1E; Figure S1D), without affecting charging by E1 (Figure S1F). The same mutations in ubiquitin blocked ubiquitination of APC/C substrates in an assay containing both Ube2C and Ube2S (Figure S1E). Thus, a noncovalent interaction with ubiquitin is required for the ability of Ube2S to assemble K11-linked ubiquitin chains.

The Hydrophobic Patch Is Required on the Donor Ubiquitin

To determine whether Ube2S interacts with donor or acceptor ubiquitin, we made a ubiquitin mutant lacking its two C-terminal Gly residues, ubi$^{\Delta GG}$. ubi$^{\Delta GG}$ is not activated by E1 and can only act as acceptor. Ube2S produced dimers between ubi$^{\Delta GG}$ and ubiquitin (ubi$^{\Delta GG}$-ubi; Figure 1F), and mutation of Lys11 on the acceptor ubi$^{\Delta GG}$, but not the donor ubiquitin, blocked this reaction (Figures 1F and 1G). The mutation of Leu8, Ile44, or Val70 on the acceptor ubi$^{\Delta GG}$ had no effect on the formation of ubi$^{\Delta GG}$-ubi dimers (Figure 1F; Figure S1G). Instead, when the hydrophobic patch was mutated on the donor ubiquitin, dimer formation was prevented (Figure 1G).

We conclude that Ube2S recognizes the *donor* ubiquitin. Several aspects of our analysis indicate that this is the only thermodynamically stable interaction between ubiquitin and Ube2S in solution. The NMR-derived binding isotherms are well described by a single-site binding model (Figure S2D); significant chemical shift perturbations map to one contiguous binding region (Figure S2B); and disruption of the donor interface did not result in the population of an alternate binding site (Figure 1B). Variation of the experimental conditions, such as ionic strength and pH, also did not provide evidence for a second binding site (data not shown). Thus, Ube2S forms a noncovalent interface with the hydrophobic patch of the donor ubiquitin, which is required for its activity to promote the formation of K11-linked ubiquitin chains.

The Donor Ubiquitin Interacts with Helix αB of Ube2S

We identified the donor-binding site on Ube2S by titrating ^{15}N-enriched UBC^{Ube2S} with ubiquitin and measuring ^{1}H-^{15}N HSQC spectra. Significant ubiquitin-induced chemical shift perturbations mapped to a surface region around the C-terminal part of helix αB of Ube2S (Figure 2A; Figure S2B). The same region was found to interact with covalently bound donor ubiquitin (Figure S2A). Mutation of two Ube2S residues in this region (C118A, I121A) impaired ubiquitin binding (Figure 2A; Figure S2C) without affecting the structural integrity of Ube2S (data not shown). The dissociation constant (K_D) for this interaction (1.11 ± 0.08 mM or 1.7 ± 0.08 mM for ubiquitin binding to UBC^{Ube2S} or Ube2S; Figure S2D) was comparable to the estimated concentration of donor ubiquitin linked to the Ube2S active site (~3 mM; Petroski and Deshaies, 2005). Our results, therefore, suggest that covalently linked donor ubiquitin occupies the noncovalent binding site on Ube2S around helix αB.

Based on our previous results, we expected the donor interface of Ube2S to be required for activity. Indeed, Ube2S^{C118A} and Ube2S^{I121A} were strongly impaired in ubi$_2$ formation (Figure 2B); K11-linked chain assembly on Ub-L-cycA with APC/C (Figure 2C); or modification of cyclin A in an APC/C assay containing Ube2C and Ube2S (Figure 2D). Disrupting this Ube2S surface did not affect charging by E1 (Figure S2E) or binding to the APC/C (Figure S2F).

To test for the importance of donor binding at physiological ubiquitin levels, we generated HeLa cell lines that stably express Ube2S or Ube2S^{I121A}. Endogenous Ube2S was specifically depleted from cells by siRNAs against the 3′ untranslated region (UTR) of the Ube2S mRNA, and formation of K11-linked chains was monitored upon exit from mitosis by a K11-linkage-specific antibody. As expected, long K11-linked chains were absent from cells lacking Ube2S, which was rescued by expression of siRNA-resistant wild-type (WT)-Ube2S (Figure 2E). By contrast, the donor-binding-deficient Ube2S^{I121A} failed to promote K11-linked chain formation. Thus, recognition of the donor ubiquitin by Ube2S is essential for K11-linked ubiquitin chain formation in vitro and in vivo.

NMR-Based Docking of the Donor Ubiquitin on Ube2S

The binding site for the donor ubiquitin on Ube2S, as defined by chemical shift mapping, makes it plausible that this interaction occurs in *cis*, i.e., involves the same E2 that the donor is covalently attached to. To test this idea, we determined whether a catalytically inactive Ube2S mutant with an intact donor-binding site (Ube2S^{C95A}) could complement the loss-of-function phenotype of a Ube2S mutant with a defective noncovalent interface (Ube2S^{C118A}, Ube2S^{I121A}). As this was not the case (Figure 2F), the observed noncovalent interaction most likely occurs in *cis*.

To obtain a structural model of the interaction between UBC^{Ube2S} and donor ubiquitin, we used the docking program HADDOCK (de Vries et al., 2007). The NMR chemical shift data were used to specify residues at the interface, and we defined only one explicit distant restraint that required the C-terminal carbon atom of Gly76 of ubiquitin to be close to the S$^{\gamma}$ atom of Cys95 in Ube2S. HADDOCK produced an ensemble of 200 structures after automated refinement, which were clustered using a backbone root-mean-square deviation (rmsd) cut-off of 7.5 Å. The resulting three clusters contain 71%, 25.5%, and 2.5% of all docked models, respectively (Table S1). As shown later, structures in cluster 1, but not those of clusters 2 and 3, could be validated by biochemical data.

As a representative structure of the Ube2S-donor ubiquitin complex, we selected a model from cluster 1 that among the top 3 according to HADDOCK scoring had the largest buried surface area, the most negative interaction energy, and the smallest number of distant restraint violations (Figure 3A; Table S1). A similar model with a low backbone rmsd of 1.1 Å was obtained by a different docking program, Cluspro (Comeau et al., 2007), without restraints (Figure S3A). Our model resembles the structure of the charged E2 Ubc9, when bound to its E3 (Reverter and Lima, 2005), and an NMR-based, docked model of the E2 Ubc1 and ubiquitin (Hamilton et al., 2001).

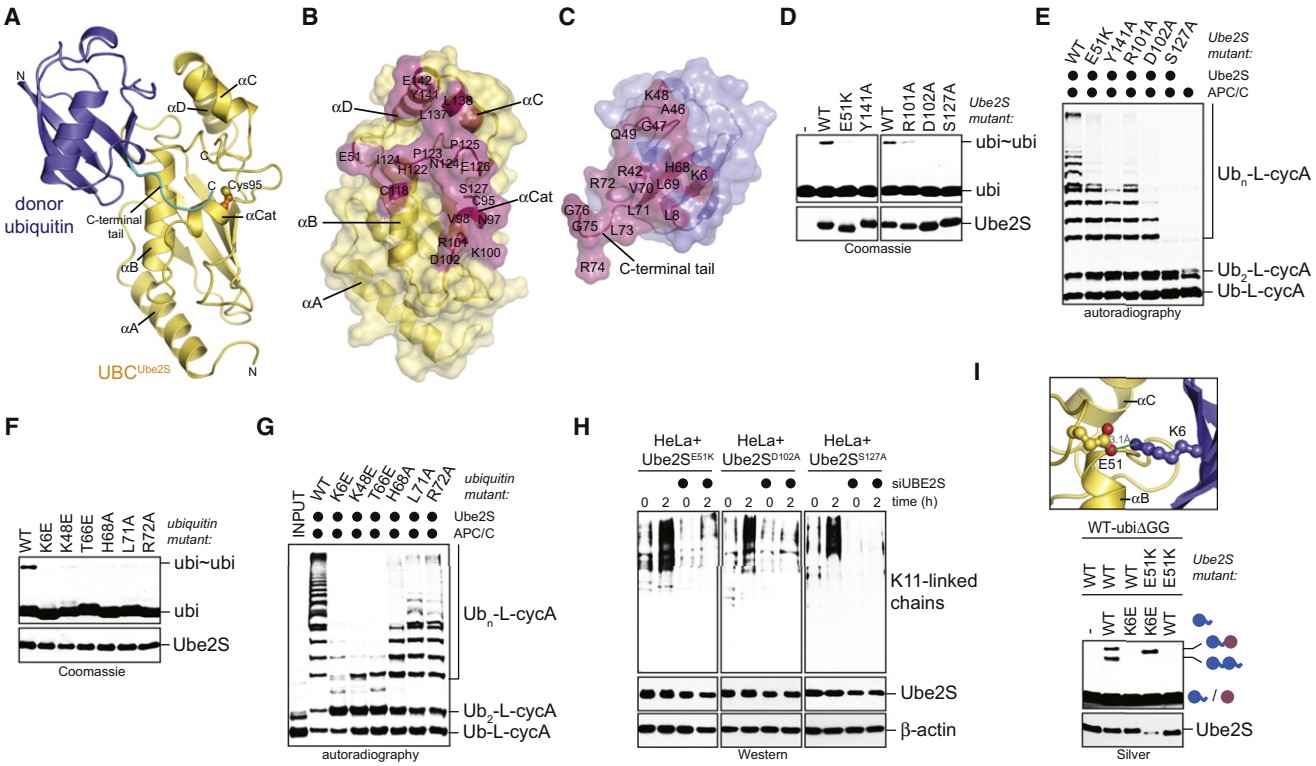

Figure 3. Structural Model of the Ube2S-Donor Ubiquitin Complex

(A) NMR-based HADDOCK model of the UBC^{Ube2S}-donor ubiquitin complex (cluster 1, no. 3; see Table S1). The C-terminal tail of ubiquitin (cyan) was allowed full flexibility during docking.

(B and C) Surface representation of the binding interface on UBC^{Ube2S} (B) and donor ubiquitin (C). Residues that make intermolecular contacts within a radius of 4 Å are shown in pink.

(D) Ube2S residues at the donor-binding interface are required for formation of ubi$_2$ dimers (ubi~ubi), as monitored by Coomassie staining.

(E) Donor-binding-deficient Ube2S mutants do not promote chain elongation on Ub-L-cycA with APC/C, as analyzed by autoradiography.

(F) Ubiquitin residues at the Ube2S interface are required for linkage formation, as seen by Coomassie staining.

(G) Ubiquitin residues at the Ube2S interface are required for chain elongation on Ub-L-cycA with APC/C, as analyzed by autoradiography.

(H) Donor binding is required for Ube2S activity in cells. HeLa cell lines expressing donor-binding-deficient Ube2S (E51K; D102A; S127A) were depleted of endogenous Ube2S, synchronized in prometaphase (t = 0) or allowed to exit mitosis (t = 2 hr), and tested for K11-linked ubiquitin chains by αK11-western.

(I) Charge-swap analysis of the ionic interaction between Lys6 of donor ubiquitin and Glu51 on Ube2S. ubi$^{\Delta GG}$ was mixed with ubiquitin or ubi^{K6E} in the presence of Ube2S or Ube2S^{E51K}. Reactions were monitored by Silver staining.

See also Figure S3 and Table S1.

Within our model, the donor ubiquitin docks onto a hydrophobic area on Ube2S, comprising the C-terminal half of helix αB, the C-terminal part of helix αC, and the N-terminal part of helix αD (Figures 3A and 3B). The corresponding interaction surface on donor ubiquitin contains the hydrophobic patch (Figure 3C), which is extended to form a contact area that buries a total of ~830 Å^2 on ubiquitin. The model includes ionic contacts between Lys6, Arg42, and Lys48 of ubiquitin, and Glu51, Glu126, and Glu142 of Ube2S (Figure S3B). An ionic contact between Arg74 of ubiquitin and Asp102 of Ube2S serves as a linchpin to guide the C terminus of ubiquitin toward the active site of Ube2S (Figure S3C). The ubiquitin tail is also anchored by hydrogen bonds between the peptide backbone and Ube2S residues close to the active site. The distance between the S$^{\gamma}$ atom of Cys95 of Ube2S and the C-terminal carbon atom of ubiquitin, 3.9 Å, is too long for a covalent bond, but small adjustments around the active site of Ube2S could readily close this gap.

Validation of the Ube2S-Donor Ubiquitin Model

Based on the selected model for this complex, we designed additional mutations to test the structural details of the predicted interface. We found that altering residues at the binding interface (Ube2S: E51K, R101A, D102A, S127A, Y141A; ubiquitin: K6E, K48E, T66E, H68A, L71A, R72A) interfered with Ube2S activity in vitro (Figures 3D–3G) and, as seen for ubi^{K6E}, disrupted the Ube2S-donor ubiquitin interaction (Figure 2A). Residues that do not make intermolecular contacts (Ube2S: D29, G30, L114, E142; ubiquitin: A46) were not required for activity (data not shown). Introducing mutations into ubi$^{\Delta GG}$ showed that most ubiquitin residues were required in the donor but not the acceptor (Figures S3D and S3E). The role of Lys6 in the acceptor ubiquitin is described below. With the exception of ubi^{R72A}, no Ube2S or ubiquitin mutant was impaired in charging by E1 (Figures S3F and S3G). To confirm this analysis in vivo, we generated cell lines that express Ube2S mutants with

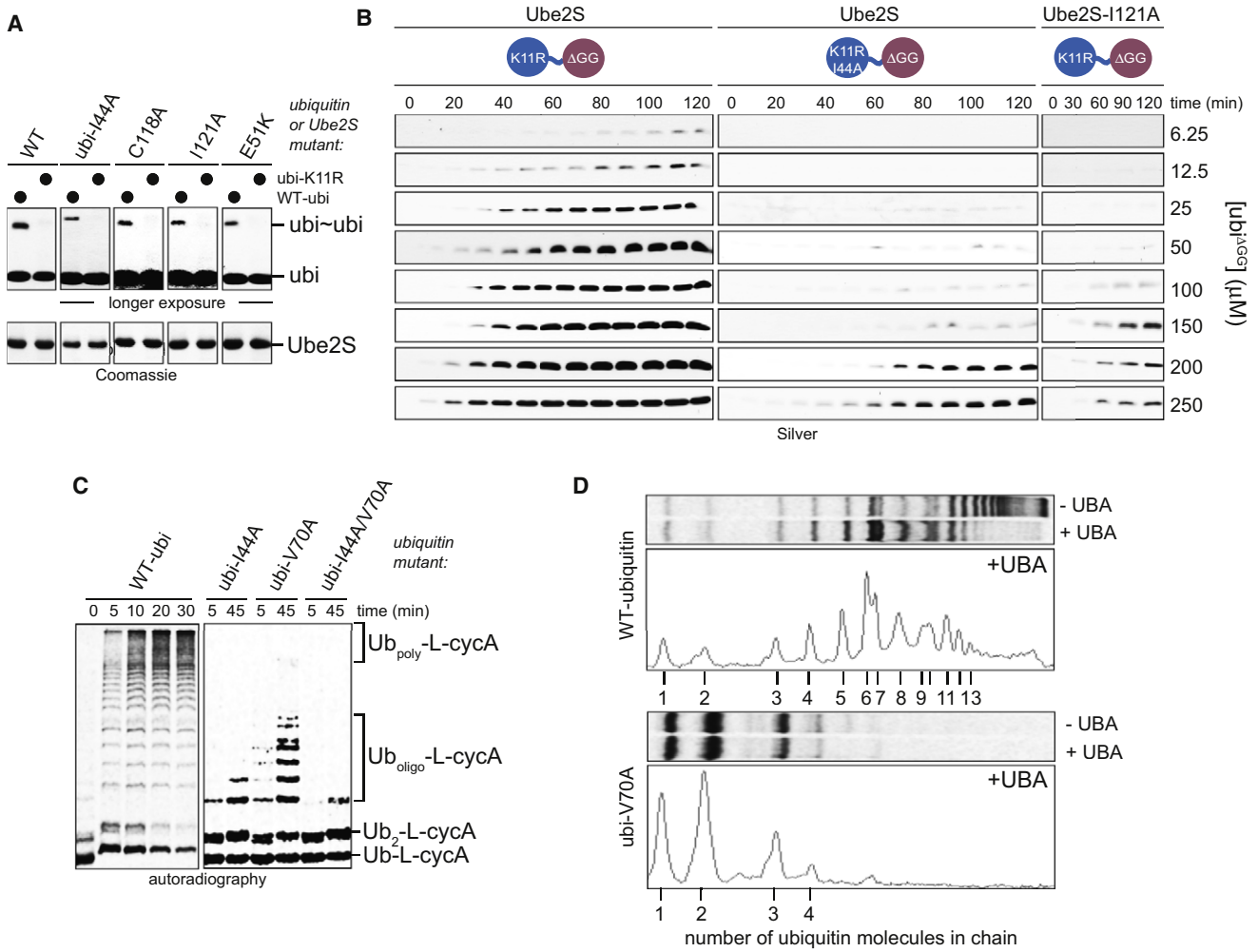

Figure 4. Noncovalent Donor Binding Increases the Processivity of Ube2S

(A) Donor binding is not required for the K11-linkage specificity of Ube2S. Ube2S or donor-binding mutants were incubated with ubiquitin or ubi^{K11R}, or as indicated with ubi^{I44A} and ubi$^{I44A/K11R}$. Reactions were incubated longer and at higher ubiquitin concentrations to observe formation of ubi$_2$ and analyzed by Coomassie staining.

(B) Donor binding promotes catalysis at low acceptor concentrations. Dimer formation between increasing levels of ubi$^{\Delta GG}$ and ubi^{K11R} or ubi$^{K11R/I44A}$, respectively, by Ube2S was monitored by Silver staining.

(C) Time-course analysis of chain elongation on Ub-L-cycA by APC/C^{Cdh1} and Ube2S in the presence of ubiquitin mutants, as analyzed by autoradiography.

(D) Donor binding is required for processive chain formation by Ube2S. Chain elongation on Ub-L-cycA by APC/C and Ube2S was monitored in the presence of the UBA domains of Rad23A. Reactions were performed with ubiquitin or ubi^{V70A} and analyzed by autoradiography (top) and line scanning (bottom).

defective donor-binding interfaces (E51K; D102A; S127A). Importantly, all of these failed to promote the formation of K11-linked ubiquitin chains in HeLa cells that lacked endogenous Ube2S (Figure 3H).

To further test our model, we used charge-swap analysis to analyze the role of the predicted ion pair between Glu51 of Ube2S and Lys6 of ubiquitin. While the K6E mutation in donor ubiquitin interfered with formation of ubi$^{\Delta GG}$-ubi dimers, this was rescued by a complementary mutation in Ube2S, Ube2S^{E51K} (Figure 3I). Ube2S^{E51K} did not establish ubi$_2$ formation for other ubiquitin mutants, such as ubi^{I44A}, attesting to the specificity of this rescue (Figure S3H). Together, the mutational studies, charge-swap analysis, and in vivo experiments validate the selected NMR-based model for the Ube2S-donor ubiquitin interaction and show its importance for chain formation by this E2.

Noncovalent Donor Ubiquitin Binding Is Required for Processive Chain Formation

We next determined the role of donor binding for catalysis by Ube2S. It was unlikely that recognizing the donor ubiquitin was important for specificity, and indeed, any ubi$_2$ formed in the presence of ubi^{I44A} was lost upon mutation of K11 (Figure 4A). The same was observed when Ube2S mutants with a defective donor-binding interface (Ube2S^{I121A}; Ube2S^{C118A}; Ube2S^{E51K}) were analyzed for ubi$_2$ formation (Figure 4A). Thus, donor binding does not determine the K11 specificity of Ube2S.

Alternatively, the noncovalent interaction between the donor and Ube2S might prevent a flexible donor molecule from interfering with acceptor recognition. If this is the case, higher concentrations of the acceptor ubi$^{\Delta GG}$ should rescue the defect in ubi$_2$ formation when the Ube2S-donor ubiquitin interface is disturbed. Consistent with this hypothesis, high levels of ubi$^{\Delta GG}$ allowed linkage formation with ubi^{I44A} or Ube2S^{I121A} (Figure 4B). The acceptor concentration required under these conditions was above the endogenous ubiquitin levels in HeLa cells (90 μM) (Ryu et al., 2006), consistent with the lack of Ube2S^{I121A} activity in vivo. These findings suggest that noncovalent binding of the donor ubiquitin facilitates acceptor recognition by Ube2S.

Based on these observations, we expected that donor binding would increase the processivity of chain formation by Ube2S. Indeed, a time-resolved analysis of chain elongation on Ub-L-cycA suggested that Ube2S assembles chains with high processivity (Figure 4C), whereas chain formation occurred in a step-like, distributive fashion if donor-binding was impaired (Figure 4C). To directly measure the processivity of chain elongation, we supplied the reactions with a UBA domain. As previously described (Rape et al., 2006), the UBA domain captures any substrate dissociating from the APC/C, thereby preventing it from rebinding the E3 and revealing the number of ubiquitin molecules transferred in a single substrate-binding event. Ube2S could transfer up to ~13 ubiquitin molecules to Ub-L-cycA per binding event (Figure 4D, top), whereas less than four molecules of the hydrophobic patch mutant ubi^{V70A} were transferred (Figure 4D, bottom). As this UBA domain only recognizes K11-chains with at least ~5 ubiquitin moieties (data not shown), the number of ubi^{V70A} molecules transferred in a single binding event is likely even smaller. Thus, the noncovalent interaction between Ube2S and donor ubiquitin increases the processivity of chain formation, at least in part by facilitating acceptor ubiquitin recognition.

Noncovalent Donor Ubiquitin Binding Is a Feature of Chain Elongation in Other E2s

To test whether other E2s bind the donor ubiquitin noncovalently, we turned to Ube2R1 and Ube2G2, which extend K48-linked chains (Li et al., 2009; Pierce et al., 2009). Disruption of the hydrophobic patch on ubiquitin strongly impaired the formation of K48 linkages by these E2s (Figure S4A), while having no effect on their charging by E1 (Figure S4B). Analogous to our results for Ube2S, we found that the activity of Ube2R1 and Ube2G2 was dependent on recognition of the hydrophobic patch on the donor but not the acceptor ubiquitin (Figure 5A). As revealed by ubi$^{I44A/K48R}$- and ubi$^{V70A/K48R}$-double mutants, noncovalent donor binding did not determine linkage specificity (Figure 5B) but was required for catalysis at low substrate concentrations (Figure 5C).

To test whether a common E2 surface recognizes the donor ubiquitin, we studied Ube2R1 mutations of sites that are structurally homologous to the Ube2S-donor interface (Figure 5D). These mutations (Ube2R1^{T122E}; Ube2R1^{L125A}; Ube2R1^{I128E}) strongly inhibited the formation of K48 linkages (Figure 5D; Figure S4C), without affecting charging by E1 (Figure S4D). The same mutations also impaired the SCF- and Ube2R1-dependent formation of ubiquitin chains on IκBα (Figure 5E). Thus, similar surfaces on the conserved E2 fold and ubiquitin are used for chain elongation by E2s of different linkage specificity. The tethering of the donor ubiquitin by an E2, therefore, provides a conserved mechanism to facilitate acceptor recognition.

Ube2S Recognizes the TEK-Box in Acceptor Ubiquitin

We next identified the binding site for the acceptor ubiquitin on Ube2S. Consistent with previous analyses (Petroski and Deshaies, 2005; Rodrigo-Brenni et al., 2010), acceptor binding was too transient to be detected by NMR, independently of whether the donor ubiquitin had been linked to the Ube2S active site or not (data not shown). We therefore used HADDOCK to dock a second ubiquitin molecule, the acceptor, onto the validated Ube2S-donor ubiquitin complex. The only restraint used for this docking defined the N$^{\zeta}$-atom of the acceptor Lys11 to be close to the S$^{\gamma}$ atom of Cys95 at the Ube2S active site. HADDOCK generated two clusters of models, which were similar in terms of energy and buried surface area (Figure S5; Table S2).

Intriguingly, models in cluster 1 orient the TEK-box of ubiquitin toward the active site of Ube2S. The TEK-box is a surface region of ubiquitin that was previously identified to mediate the preference of Ube2C/UbcH10 for assembling K11-linked chains (Jin et al., 2008). We found that mutation of the TEK-box strongly interfered with the ability of Ube2S to synthesize K11-linked ubi$_2$ (Figure 6A), to elongate chains on Ub-L-cycA (Figure 6B), and to modify cyclin A in a full APC/C assay (Figure S6A). Residues outside of the TEK-box (Thr9, Glu16, Lys33) were not required for activity (data not shown). Introducing mutations into ubi$^{\Delta GG}$ revealed that the TEK-box was essential on the acceptor (Figure 6C) but, with exception of Lys6, not the donor ubiquitin (Figure 6D). The TEK-box was dispensable for Ube2S charging by E1 (Figure S6B) or binding of donor ubiquitin to Ube2S (Figure S6C). Thus, the TEK-box of the acceptor ubiquitin is required for K11-linkage formation by Ube2S.

On the basis of these results, we performed another docking run that defined four TEK-box residues to be at the interface (Table S2). All HADDOCK solutions grouped into a single cluster reproducing the binding topology of cluster 1 of the previous run (Figure 6E). With backbone rmsd values of ~1 Å, the best models of this ensemble were remarkably similar, and we focused on the top-scoring model (cluster 1, no. 1; Table S2, bottom).

In this model of the ternary complex, the acceptor ubiquitin interacts mostly with Ube2S (Figure 6E), with a total buried surface area between the acceptor ubiquitin and the Ube2S-donor complex of ~980 Å^2 (Figures 6F and 6G). The acceptor ubiquitin uses its β strand region to bind a surface of Ube2S comprising the active site helix αCat, the loop region between helices αB and αC, and helix αC (Figure 6F). Although the interaction leads to the burial of few hydrophobic residues, these are not closely packed, and the interface is predominantly electrostatic. In particular, a network of ionic contacts involving Lys6 and Lys63 of ubiquitin, Glu131 and Glu139 of Ube2S, and a series of hydrogen bonds including Glu64 of ubiquitin and Arg135 of Ube2S are key features of the interface (Figure S6D). The electrostatic Ube2S-acceptor interface is consistent with the low affinity between these molecules (Sheinerman and Honig, 2002).

Mutating residues in the predicted binding site on Ube2S (N97A, E131K, R135E), but not outside of this interface (K76,

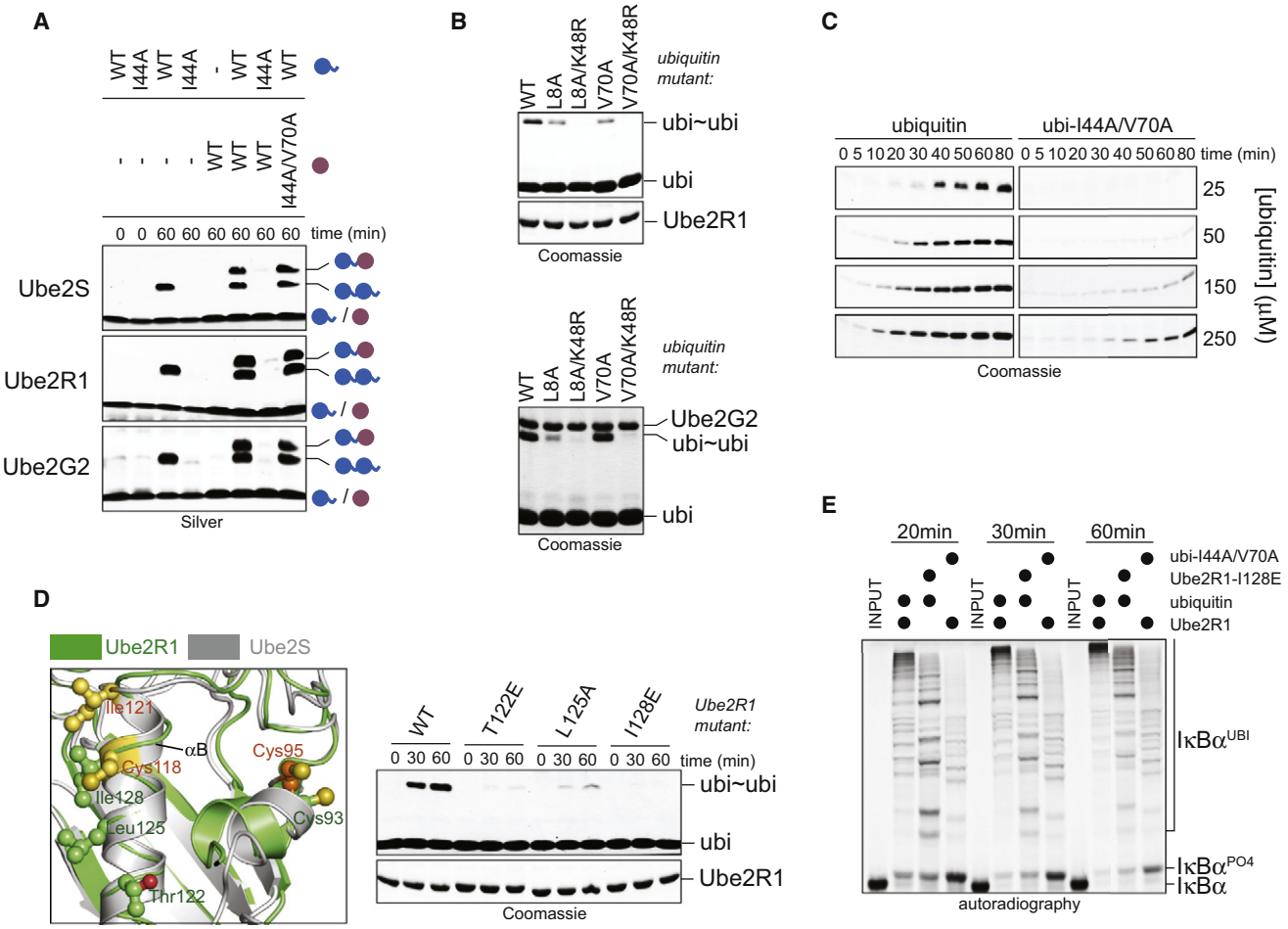

Figure 5. Noncovalent Donor Binding Is Utilized by E2s Independently of Linkage Specificity

(A) Ube2R1 and Ube2G2 require the hydrophobic patch in the donor but not acceptor ubiquitin for K48-linkage formation. Ube2S, Ube2R1, or Ube2G2 and its E3 gp78 were incubated with $ubi^{\Delta GG}$ or $ubi^{\Delta GG/I44A/V70A}$ (purple) and ubiquitin or ubi^{I44A} (blue). Reactions were analyzed by Silver staining.

(B) The hydrophobic patch of donor ubiquitin is not required for K48 specificity of Ube2R1 or Ube2G2. ubi_2 formation by Ube2R1 or Ube2G2/gp78 with ubiquitin mutants was analyzed by Coomassie staining.

(C) Donor binding is required for rapid catalysis by Ube2R1. Time courses of ubi_2 formation by Ube2R1 in the presence of increasing concentrations of ubiquitin or ubi^{I44A} were analyzed by Coomassie staining.

(D) A similar surface as the donor-binding interface of Ube2S (yellow) is required in Ube2R1 (green; PDB ID: 2OB4). Ube2R1 mutants were analyzed for K48-specific ubi_2 formation by Coomassie staining.

(E) Donor binding is required for processive chain formation by $SCF^{\beta TrCP}$ and Ube2R1. Phosphorylated IκBα was incubated with $SCF^{\beta TrCP}$, Ube2R1 or $Ube2R1^{I128E}$, and ubiquitin or $ubi^{I44A/V70A}$ and analyzed by autoradiography.

See also Figure S4.

N91, E93, K100, E126, E132), impaired production of ubi_2 (Figure 6H; data not shown), chain elongation on Ub-L-cycA (Figure 6I), and substrate modification in a full APC/C assay (Figure S6E). As seen in cells expressing $Ube2S^{E131K}$ or $Ube2S^{R135E}$, these mutations also inhibited formation of K11-linked chains in vivo (Figure 6J). Asn97, Glu131, and Arg135 were not required for Ube2S charging by E1 (Figure S6F) or Ube2S binding to the APC/C (Figure S2F).

We next probed the predicted ionic contacts between Ube2S and the acceptor ubiquitin by charge-swap analyses. Our model found the acceptor Lys6 to face Glu131 of Ube2S (Figure 7A). Consistent with this, the loss of $ubi^{\Delta GG}$-ubi formation caused by a K6E mutation in the acceptor $ubi^{\Delta GG}$ could be rescued by $Ube2S^{E131K}$ or $Ube2S^{E131A}$ (Figure 7A; Figure S7A), but not by other Ube2S mutants in this interface (N97A, R135E) (Figure S7B). Thus, the acceptor Lys6 is recognized by Glu131 of Ube2S, whereas the donor Lys6 contacts Glu51 of Ube2S (Figure 3); indeed, $Ube2S^{E51K/E131K}$ completely rescued ubi_2 formation by ubi^{K6E} (Figure 7B; Figure S7C). Our model also showed Arg135 of Ube2S in proximity of Glu64 of ubiquitin. Accordingly, the diminished activity of $Ube2S^{R135E}$ was significantly rescued by ubi^{E64K} (Figure S7D), but not other ubiquitin mutants in the proximity of this surface (Figure S7E). Finally, less ubi_2 was formed in the presence of ubi^{K63E}, which could be rescued by

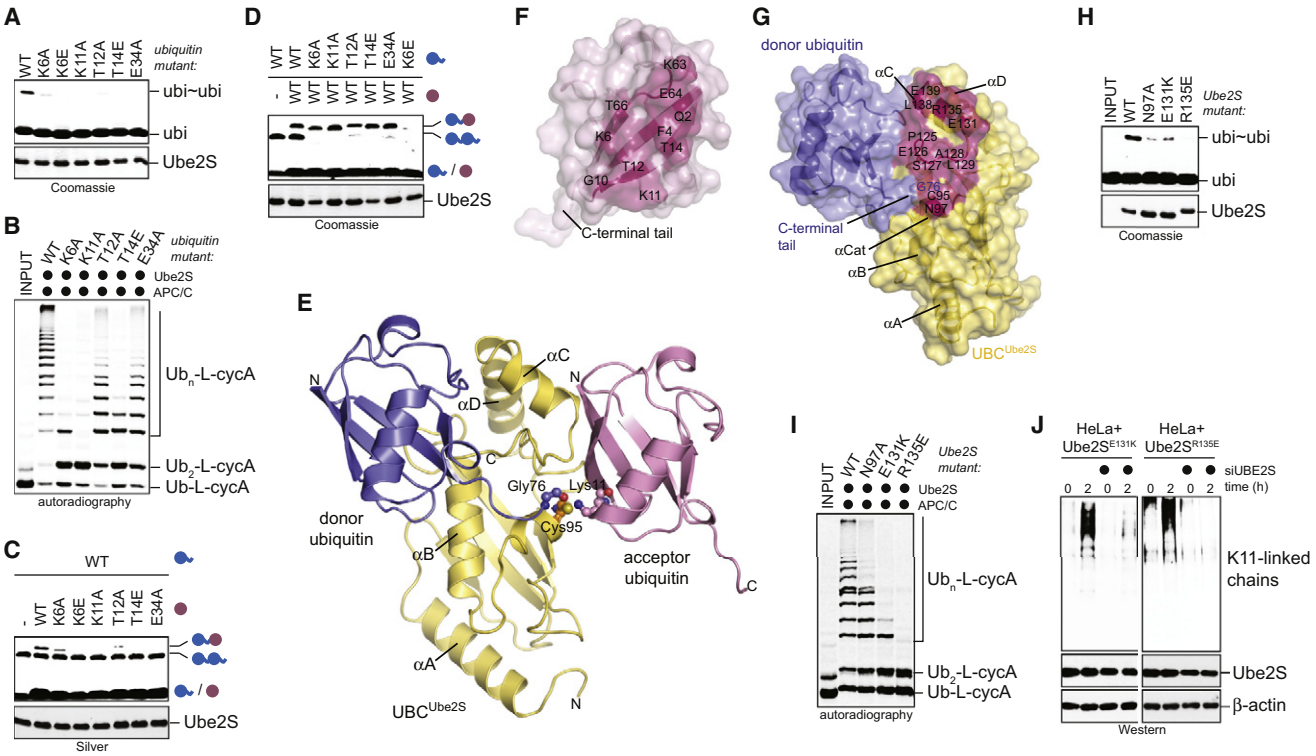

Figure 6. Acceptor Ubiquitin Recognition by the Ube2S-Donor Ubiquitin Complex

(A) The TEK-box in ubiquitin is required for K11-linkage formation by Ube2S. Ube2S was incubated with ubiquitin mutants, and ubi$_2$ formation (ubi~ubi) was monitored by Coomassie staining.

(B) TEK-box mutants in ubiquitin inhibit chain formation on Ub-L-cycA by Ube2S and APC/C, as analyzed by autoradiography.

(C) The TEK-box is required on acceptor ubiquitin. ubi$^{\Delta GG}$ mutants (purple) were incubated with ubiquitin (blue) and Ube2S and analyzed by Silver staining.

(D) The TEK-box is not required in donor ubiquitin. TEK-box mutants of ubiquitin were mixed with WT-ubi$^{\Delta GG}$ and Ube2S, and reactions were analyzed by Coomassie staining.

(E) HADDOCK-based model of the ternary complex between the UBC^{Ube2S} (yellow), donor ubiquitin (blue), and acceptor ubiquitin (pink; cluster 1, no. 1; see Table S2, bottom).

(F) Surface representation of the Ube2S-binding interface on acceptor ubiquitin. Contact residues within a radius of 4 Å are shown in pink.

(G) Surface representation of the acceptor-binding interface on the Ube2S-donor complex.

(H) Acceptor binding is required for Ube2S activity. Ube2S mutants were incubated with ubiquitin and analyzed by Coomassie staining.

(I) Ube2S residues at the acceptor interface are required for chain elongation by APC/C. The modification of Ub-L-cycA by APC/C and Ube2S mutants was analyzed by autoradiography.

(J) Ube2S residues at the acceptor-binding interface are required in vivo. HeLa cell lines expressing Ube2S^{E131K} and Ube2S^{R135E} were treated with siRNAs to deplete endogenous Ube2S, arrested in prometaphase (t = 0 hr) or allowed to exit mitosis (t = 2 hr), and tested for K11-linked chains by αK11-western.

See also Figure S5, Figure S6, and Table S2.

mutation of the opposing Glu139 of Ube2S (Figure S7F). The mutational and charge-swap analyses provide strong support for our model of acceptor recognition by Ube2S.

Linkage Specificity Is Determined by Substrate-Assisted Catalysis

The low affinity of Ube2S for acceptor ubiquitin raised the question of how this E2 achieves the stringent selection of K11 over other linkages. In one scenario, recognition of other Lys residues would be even less favored, with differences in binding energies accounting for the K11 specificity of Ube2S. To address this issue, we carried out docking calculations that placed each of the other Lys residues of ubiquitin in proximity to the active site of charged Ube2S. Among the clusters returned by HADDOCK, several had buried surface areas and energy characteristics comparable to our K11-centered model (Figure S8; Table S3). This suggests that other Lys residues can be exposed to the active site of Ube2S, yet these binding events do not result in linkage formation. Thus, selective acceptor binding is not sufficient to explain the K11 specificity of Ube2S.

Alternatively, the composition of the active site of Ube2S might force the reaction toward K11 linkages. Our models of the ternary complex found that the active site of Ube2S was similar to the E2 Ubc9 (Reverter and Lima, 2005; Figure 7C). For Ubc9, several residues in addition to the active site cysteine were attributed roles in catalysis: Tyr87 and Asn85 of Ubc9 contribute to pK_a suppression of the substrate lysine through desolvation. Further, Asn85 serves to stabilize the oxyanion intermediate during ubiquitin transfer, and Tyr87 provides a hydrophobic

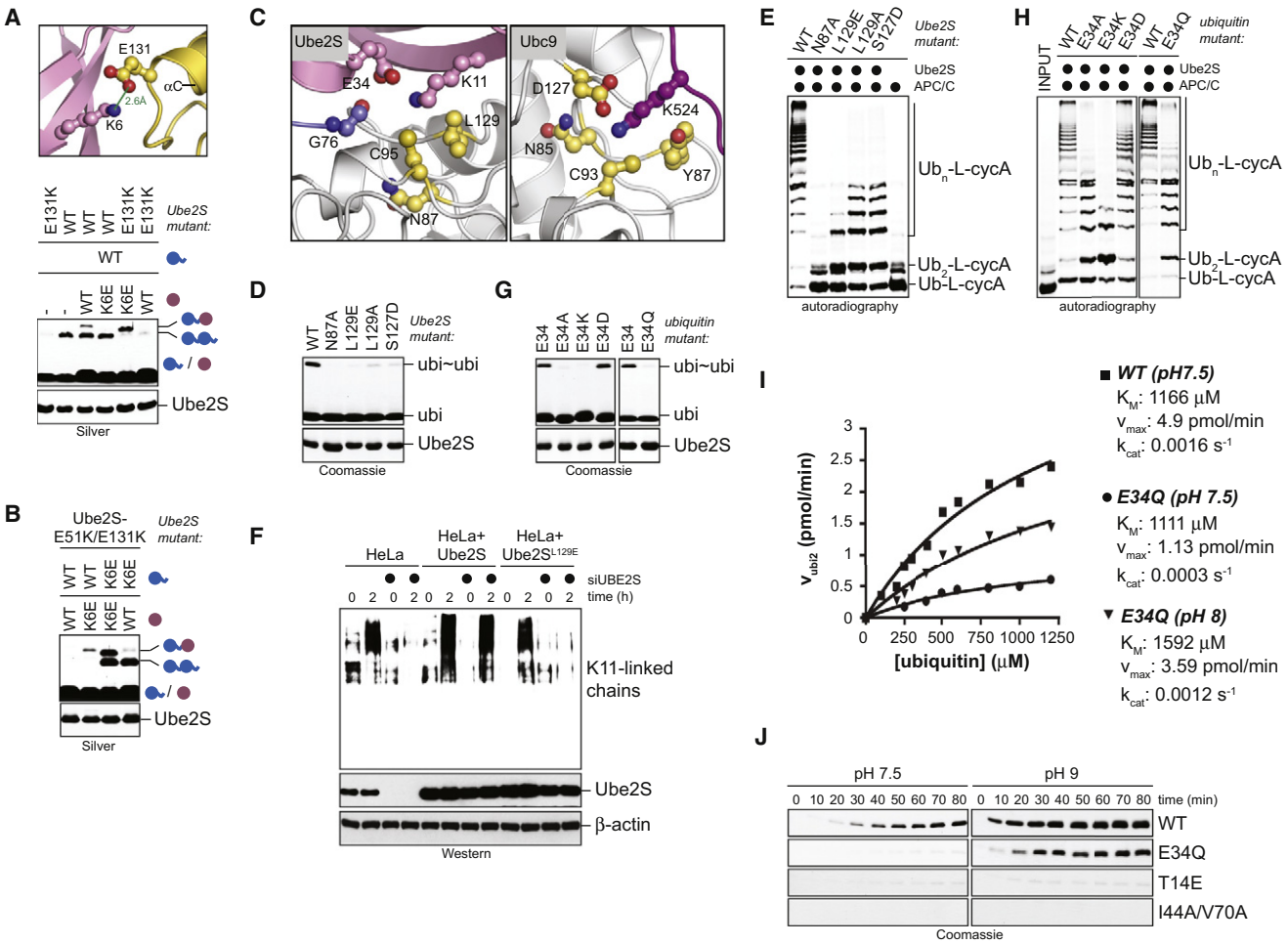

Figure 7. Substrate-Assisted Catalysis Contributes to the K11-Linkage Specificity of Ube2S

(A) Charge-swap analysis of the ionic contact between acceptor Lys6 and Glu131 of Ube2S. Ube2S or Ube2S^{E131K} was mixed with ubi$^{\Delta GG}$ or ubi$^{\Delta GG/K6E}$ and reactions were analyzed by Silver staining.

(B) Ube2S$^{E51K/E131K}$ rescues mutation of Lys6 in both acceptor and donor ubiquitin. Lys6 was mutated in acceptor ubi$^{\Delta GG}$ (purple) or donor ubiquitin (blue), and ubi$^{\Delta GG}$-ubi formation by Ube2S or Ube2S$^{E51K/E131K}$ was analyzed by Silver staining.

(C) Ube2S (left) and Ubc9 (PDB ID: 2GRN; right) show similar active site constellations. The highest scoring Ube2S model of the HADDOCK run in the absence of ambiguous restraints is shown (Table S2, top; cluster 1, no 1).

(D) Candidate active-site residues are required for the activity of Ube2S to catalyze ubi$_2$ formation (ubi~ubi), as analyzed by Coomassie staining.

(E) Active-site residues in Ube2S are required for chain elongation by APC/C. Ub-L-cycA was incubated with APC/C^{Cdh1} and Ube2S mutants and analyzed by autoradiography.

(F) Leu129 is required for Ube2S activity in vivo. HeLa cell lines expressing Ube2S or Ube2S^{L129} were tested for formation of K11-linked chains after endogenous Ube2S was depleted by siRNAs. K11-chain formation in cells arrested in prometaphase or exiting mitosis was monitored by αK11-western.

(G) Glu34 of acceptor ubiquitin is required for K11-linkage formation. Ubiquitin mutants were incubated with Ube2S and analyzed by Coomassie staining.

(H) Glu34 of acceptor ubiquitin is required for chain elongation by APC/C and Ube2S. The modification of Ub-L-cycA by APC/C, Ube2S, and ubiquitin mutants was analyzed by autoradiography.

(I) ubi^{E34Q} displays catalytic, but not binding defects. The rates of ubi$_2$ formation at different concentrations of ubiquitin and ubi^{E34Q} at the indicated pH were determined from two or three independent time courses. Apparent kinetic constants were obtained by fitting the rate constants to a Michaelis-Menten equation.

(J) Rescue of ubi^{E34Q}, but not other TEK-box or hydrophobic patch mutants, by increasing the reaction pH. Ubiquitin or indicated mutants were incubated with Ube2S at pH 7.5 (left) or pH 9 (right) and analyzed by Coomassie staining.

See also Figure S7, Figure S8, and Table S3.

platform to position the attacking lysine side chain (Yunus and Lima, 2006). Whereas Asn85 of Ubc9 is conserved in Ube2S (Asn87) (Figure 7C), the attacking lysine is likely positioned by Leu129 of Ube2S (Figure 7C). Asn87 and Leu129 are essential for Ube2S activity in vitro (Figures 7D and 7E) and, as seen with HeLa cell lines expressing Ube2S^{L129E}, in vivo (Figure 7F). The mutation of Asn87 or Leu129 did not impede charging of Ube2S by E1 (Figure S7G).

In addition to Asn85 and Tyr87, Asp127 of Ubc9 was assigned a catalytic role in reducing the pK_a of the substrate lysine (Yunus

and Lima, 2006). In Ube2S, this residue is replaced by serine (Ser127), which our models place into a position to interact with the donor ubiquitin rather than activate an acceptor lysine (Figure 3). Strikingly, instead of an E2 residue, our models show an amino acid of ubiquitin, Glu34, to be in an appropriate position to orient the acceptor Lys11 and to promote its desolvation (Figure 7C). The mutation of Glu34 inhibited K11-linkage formation (Figures 7G and 7H), and kinetic analyses found this to be due to a strong reduction in the apparent catalytic rate constant (k_{cat}) but not the Michaelis-Menten constant (K_M) (Figure 7I). Thus, a residue in the substrate, Glu34 of ubiquitin, plays an important role in catalysis by Ube2S.

Due to its position in the ternary complex, Glu34 is expected to orient Lys11, but not other Lys residues, and to suppress its pK_a. The E34Q mutant of ubiquitin might maintain the position of Lys11 but fail to promote its deprotonation. If this assumption is correct, the inability of ubi^{E34Q} to produce ubi_2 may be rescued by increasing the pH of the reaction, which facilitates lysine deprotonation. Indeed, Ube2S efficiently linked ubi^{E34Q} molecules at higher pH (Figure 7J), which was due to a change in the apparent k_{cat}, but not K_M (Figure 7I). By contrast, an acceptor TEK-box mutant defective in Ube2S binding (ubi^{T14E}) and a donor ubiquitin mutant ($ubi^{I44A/V70A}$) were inactive at pH 9 (Figure 7J). These findings support the notion that Glu34 of ubiquitin participates in catalysis by suppressing the pK_a of the acceptor Lys11.

As the catalytic role of Glu34 could be bypassed by increasing the pH, the same treatment might reduce the specificity of Ube2S. Consistent with this hypothesis, Ube2S modified Lys residues in a peptide derived from its C-terminal tail much more efficiently at pH 9 than at pH 7.5 (Figure S7H). Moreover, at pH 9, but not at pH 7.5, Lys63 and Lys48 of ubiquitin could act as acceptor for Ube2S (Figure S7I), although the bulk of linkage formation still occurred through K11 (Figure S7J). These findings further suggest that Ube2S requires a residue in ubiquitin, Glu34, for specific formation of K11 linkages. We conclude that Ube2S promotes linkage-specific ubiquitin chain formation by substrate-assisted catalysis.

Conclusions

K11- and K48-linked ubiquitin chains are often assembled by single-subunit E2s that cooperate with RING-E3s (Ye and Rape, 2009). Most of these E2s are specific and processive, but how these properties are achieved in the absence of cofactors was poorly understood. Here, we addressed this question by dissecting the mechanism of ubiquitin chain assembly by the K11-specific E2 Ube2S.

We found that Ube2S requires a noncovalent interaction with the donor ubiquitin for chain formation. Although the affinity of Ube2S for the donor ubiquitin is weak, this interaction occurs in addition to the covalent thioester bond at the E2 active site. It tethers the donor ubiquitin to the E2, thereby restricting its flexibility and facilitating acceptor recognition. It also places the C terminus of the donor ubiquitin in an optimal position for nucleophilic attack by the acceptor lysine.

The Ube2S-donor ubiquitin complex binds the acceptor ubiquitin very transiently through primarily electrostatic interactions. Ube2S recognizes the TEK-box on acceptor ubiquitin, a motif previously identified as being required for formation of K11 linkages by Ube2C (Jin et al., 2008). As seen in crystal structures of K11-linked ubiquitin dimers (Matsumoto et al., 2010; Bremm et al., 2010), all TEK-box residues in the distal ubiquitin are fully accessible for recognition by Ube2S.

The low affinity of Ube2S for the acceptor is in agreement with observations for other E2s (Petroski and Deshaies, 2005; Rodrigo-Brenni et al., 2010) and likely protects cells from spurious chain elongation in the absence of E3s. However, together with our comparative docking analysis, the transient nature of acceptor binding suggests that selective acceptor recognition does not explain the linkage specificity of Ube2S.

Indeed, our model of the ternary complex between Ube2S, donor, and acceptor ubiquitin revealed that Ube2S lacks a residue required for suppressing the pK_a of the substrate lysine. This function is instead provided by Glu34 of ubiquitin, which is in direct proximity to Lys11. Mutation of Glu34 had strong effects on the apparent k_{cat}, but not the K_M, of linkage formation by Ube2S, supporting a role in catalysis. Other Lys residues of ubiquitin do not have a suitably positioned acidic residue when docked into the active site of Ube2S or display features incompatible with catalysis (Figure S8). The same likely applies to Lys residues of APC/C substrates, which may explain why Ube2S is unable to promote chain initiation (Garnett et al., 2009; Williamson et al., 2009). Thus, our findings suggest that formation of a competent catalytic center requires residues of Ube2S and ubiquitin, which only occurs when K11 of the acceptor is exposed to the active site of Ube2S. We conclude that linkage-specific chain assembly by Ube2S occurs through substrate-assisted catalysis.

Do other E2 enzymes use similar mechanisms for ubiquitin transfer? We found that noncovalent donor binding is a property shared by E2s with different linkage specificity. Ube2R1 and Ube2G2 also tether the donor ubiquitin for efficient catalysis, but not for K48 specificity, and Ube2R1 uses a similar surface on its UBC domain as Ube2S uses for donor recognition. In addition, the HECT-E3 Nedd4L binds E2-linked donor ubiquitin, a feature required for rapid ubiquitin transfer to the catalytic cysteine of the E3 (Kamadurai et al., 2009); the E3 RanBP2 binds SUMO to restrict its conformational freedom (Reverter and Lima, 2005); and in some cases, a ubiquitin-binding domain can promote E2-dependent ubiquitination reactions (Hoeller et al., 2007). We, therefore, propose that noncovalent donor binding is a general property of ubiquitination enzymes to increase the processivity of substrate modification.

Other E2s may also use substrate-assisted catalysis for chain assembly. Mms2-Ubc13 positions Glu64 of ubiquitin close to the E2 active site, and mutation of this residue resulted in a decrease of K63-linkage formation (Eddins et al., 2006). Thus, although acceptor binding to Mms2 helps to orient Lys63 toward the active site of Ubc13, a catalytic ubiquitin residue might increase the specificity of chain formation. Moreover, mutation of a Tyr residue in ubiquitin reduced the catalytic rate of K48-linkage formation by yeast Ubc1 (Rodrigo-Brenni et al., 2010). Together, these findings allow us to propose that several E2 enzymes achieve linkage-specific ubiquitin chain formation through a mechanism of substrate-assisted catalysis.

EXPERIMENTAL PROCEDURES

A detailed methods description can be found in the Extended Experimental Procedures.

Reagents

Table S4 shows a complete list of all constructs.

Protein Purification

Most proteins were purified from BL21/DE3 (RIL) cells. E1 was purified from Sf9 cells. For uniform isotopic enrichment, Ube2S and ubiquitin were expressed in M9-medium using ^{15}N-enriched $(NH_4)_2SO_4$ and/or ^{13}C-enriched glucose.

To generate ester-linked complex, 75 μM ^{15}N-enriched UBC$^{Ube2S/C95S}$ and 230 μM unlabeled ubiquitin were incubated at 37°C for 3 hr. The diluted reaction was subjected to two rounds of anion-exchange chromatography.

Formation of ubi$_2$

60 μM ubiquitin and/or ubi$^{\Delta GG}$ and 5 μM E2s were incubated with E1 and energy mix at 30°C for 1 hr and analyzed by Coomassie or Silver staining. In assays comparing activity at different pH, Tris/HCl was replaced with 50 mM Bis-tris propane, pH 7.5, 8, or 9.

Ube2S Kinetics Assays

Time courses of ubi$_2$ formation were performed with different concentrations of WT- or E34Q-ubiquitin. Levels of ubi$_2$ were quantified by Quantity One and compared to a known amount of Ube2S on each gel. Initial velocity rates and kinetic constants were calculated with GraphPad Prism and Michaelis-Menten equations.

APC/C Ubiquitination Assays

^{35}S substrates were synthesized by IVT/T. Ub-L-cycA was synthesized in the presence of 175 μM ubi^{K29R} to inhibit the UFD-pathway, which is active in reticulocyte lysate. To purify ^{35}S-Ub-L-cycA, ^{His}Cdk2 was bound to NiNTA. IVT/T was added to beads for 3 hr at 4°C. Beads were eluted with imidazole, and Ub-L-cycA/Cdk2-complexes were concentrated with 30 MWCO Microcon filters. APC/C was purified from G1-HeLa extracts and used for ubiquitination as described (Rape et al., 2006).

Analysis of Ube2S Activity In Vivo

HeLa cells were transfected in 6-well plates with 4 μg Ube2S vectors and Lipofectamine 2000. Twenty-four hours later, 10% of transfected cells were expanded to 10 cm dishes and selected with hygromycin B. Individual hygromycin-resistant colonies were picked with cloning discs and tested for Ube2S expression by western.

Cells expressing Ube2S or mutants were transfected with 100 nM siRNA with Oligofectamine and synchronized in prometaphase by thymidine/nocodazole. Samples were taken at 0 hr and 2 hr post-release and processed for αK11-western.

Computational Docking

Donor docking was performed with HADDOCK 2.1, using crystal structures of UBC^{Ube2S} (Protein Data Bank (PDB) ID: 1ZDN, chain A) and ubiquitin (PDB ID: 1UBQ). Active residues were based on chemical shift perturbation data and solvent accessibility. For thioester linkage between donor and Ube2S, we applied an unambiguous intermolecular distance restraint between C95 of Ube2S and G76 of ubiquitin. Residues 70–76 of ubiquitin were defined fully flexible.

To generate a model of the ternary complex, we docked a second ubiquitin onto the selected E2-donor complex (cluster 1, no. 3; Table S1). We initially applied a single unambiguous restraint between K11 of the acceptor and C95 of Ube2S (Table S2, top), followed by a refined run with ambiguous restraints based on functional data (Table S2).

Additional donor-docking experiments used ClusPro 2.0 and default parameters.

NMR

Data were recorded at 25°C on Bruker DRX spectrometers (500, 600, 800, and 900 MHz) and processed with NMRPipe. Backbone chemical shift assignments for UBC^{Ube2S} and ubiquitin were obtained by standard triple resonance experiments. Titration experiments were performed by mixing stock solutions containing 240 μM ^{15}N-enriched UBC^{Ube2S} or 200 μM ^{15}N-enriched ubiquitin and no or an ~6-fold molar excess of unlabeled partner. Phase-sensitive gradient-enhanced ^{1}H-^{15}N HSQC spectra were recorded. To compare chemical shift perturbations, a weighted combined chemical shift difference $\Delta\delta(^{1}H^{15}N)$ was calculated.

^{1}H-^{15}N HSQC experiments of ester-linked complex between ^{15}N-enriched UBC$^{Ube2S/C95S}$ and ubiquitin were recorded with 22 μM complex.

ACCESSION NUMBERS

The 1H, 15N, and 13C backbone chemical shift assignments for Ube2S (1–156) and ubiquitin have been submitted to the Biological Magnetic Resonance Bank (BMRB), http://www.bmrb.wisc.edu, with accession numbers 17437 and 17439, respectively.

SUPPLEMENTAL INFORMATION

Supplemental Information includes Extended Experimental Procedures, eight figures, and four tables and can be found with this article online at doi:10.1016/j.cell.2011.01.035.

ACKNOWLEDGMENTS

We thank H.J. Meyer for Ub-L-cycA; A. Williamson for golden extracts; members of the Rape and Kuriyan labs, J. Winger, S. Kassube, and J. Kirsch for discussions; J. Schaletzky for reading the manuscript and suggestions; J. Pelton for help with NMR experiments; D. King and T. Iavarone for mass spectrometry; and the staff at beamline 12.3.1 at LBNL for technical support. NMR instrumentation and operation were supported by NIH-GM 68933, NIH GM68933, NSF BBS 0119304 and NIH RR15756, and NSF BBS 8720134. S.L. is a fellow of The Leukemia & Lymphoma Society. M.R. is a Pew fellow and is supported by NIH GM83064 and an NIH New Innovator Award.

Received: July 8, 2010
Revised: November 24, 2010
Accepted: January 31, 2011
Published: March 3, 2011

REFERENCES

Bremm, A., Freund, S.M., and Komander, D. (2010). Lys11-linked ubiquitin chains adopt compact conformations and are preferentially hydrolyzed by the deubiquitinase Cezanne. Nat. Struct. Mol. Biol. *17*, 939–947.

Comeau, S.R., Kozakov, D., Brenke, R., Shen, Y., Beglov, D., and Vajda, S. (2007). ClusPro: Performance in CAPRI rounds 6-11 and the new server. Proteins *69*, 781–785.

Deshaies, R.J., and Joazeiro, C.A. (2009). RING-domain E3 ubiquitin ligases. Annu. Rev. Biochem. *78*, 399–434.

de Vries, S.J., van Dijk, A.D., Krzeminski, M., van Dijk, M., Thureau, A., Hsu, V., Wassenaar, T., and Bonvin, A.M. (2007). HADDOCK versus HADDOCK: new features and performance of HADDOCK2.0 on the CAPRI targets. Proteins *69*, 726–733.

Dikic, I., Wakatsuki, S., and Walters, K.J. (2009). Ubiquitin-binding domains - from structures to functions. Nat. Rev. Mol. Cell Biol. *10*, 659–671.

Eddins, M.J., Carlile, C.M., Gomez, K.M., Pickart, C.M., and Wolberger, C. (2006). Mms2-Ubc13 covalently bound to ubiquitin reveals the structural basis of linkage-specific polyubiquitin chain formation. Nat. Struct. Mol. Biol. *13*, 915–920.

Garnett, M.J., Mansfeld, J., Godwin, C., Matsusaka, T., Wu, J., Russell, P., Pines, J., and Venkitaraman, A.R. (2009). UBE2S elongates ubiquitin chains on APC/C substrates to promote mitotic exit. Nat. Cell Biol. *11*, 1363–1369.

Hamilton, K.S., Ellison, M.J., Barber, K.R., Williams, R.S., McKenna, S., Ptak, C., Glover, M., and Shaw, G.S. (2001). Structure of a conjugating

enzyme-ubiquitin thiolester intermediate reveals a novel role for the ubiquitin tail. Structure *9*, 897–904.

Hoeller, D., Hecker, C.M., Wagner, S., Rogov, V., Dötsch, V., and Dikic, I. (2007). E3-independent monoubiquitination of ubiquitin-binding proteins. Mol. Cell *26*, 891–898.

Jin, L., Williamson, A., Banerjee, S., Phillip, I., and Rape, M. (2008). Mechanism of ubiquitin chain formation by the human Anaphase-Promoting Complex. Cell *133*, 653–665.

Jung, C.R., Hwang, K.S., Yoo, J., Cho, W.K., Kim, J.M., Kim, W.H., and Im, D.S. (2006). E2-EPF UCP targets pVHL for degradation and associates with tumor growth and metastasis. Nat. Med. *12*, 809–816.

Kamadurai, H.B., Souphron, J., Scott, D.C., Duda, D.M., Miller, D.J., Stringer, D., Piper, R.C., and Schulman, B.A. (2009). Insights into ubiquitin transfer cascades from a structure of a UbcH5B approximately ubiquitin-HECT (NEDD4L) complex. Mol. Cell *36*, 1095–1102.

Li, W., Tu, D., Li, L., Wollert, T., Ghirlando, R., Brunger, A.T., and Ye, Y. (2009). Mechanistic insights into active site-associated polyubiquitination by the ubiquitin-conjugating enzyme Ube2g2. Proc. Natl. Acad. Sci. USA *106*, 3722–3727.

Matsumoto, M.L., Wickliffe, K.E., Dong, K.C., Yu, C., Bosanac, I., Bustos, D., Phu, L., Kirkpatrick, D.S., Hymowitz, S.G., Rape, M., et al. (2010). K11-linked polyubiquitination in cell cycle control revealed by a K11 linkage-specific antibody. Mol. Cell *39*, 477–484.

Petroski, M.D., and Deshaies, R.J. (2005). Mechanism of lysine 48-linked ubiquitin-chain synthesis by the cullin-RING ubiquitin-ligase complex SCF-Cdc34. Cell *123*, 1107–1120.

Pierce, N.W., Kleiger, G., Shan, S.O., and Deshaies, R.J. (2009). Detection of sequential polyubiquitylation on a millisecond timescale. Nature *462*, 615–619.

Rape, M., Reddy, S.K., and Kirschner, M.W. (2006). The processivity of multiubiquitination by the APC determines the order of substrate degradation. Cell *124*, 89–103.

Reverter, D., and Lima, C.D. (2005). Insights into E3 ligase activity revealed by a SUMO-RanGAP1-Ubc9-Nup358 complex. Nature *435*, 687–692.

Rodrigo-Brenni, M.C., Foster, S.A., and Morgan, D.O. (2010). Catalysis of lysine 48-specific ubiquitin chain assembly by residues in E2 and ubiquitin. Mol. Cell *39*, 548–559.

Ryu, K.Y., Baker, R.T., and Kopito, R.R. (2006). Ubiquitin-specific protease 2 as a tool for quantification of total ubiquitin levels in biological specimens. Anal. Biochem. *353*, 153–155.

Schulman, B.A., and Harper, J.W. (2009). Ubiquitin-like protein activation by E1 enzymes: the apex for downstream signalling pathways. Nat. Rev. Mol. Cell Biol. *10*, 319–331.

Sheinerman, F.B., and Honig, B. (2002). On the role of electrostatic interactions in the design of protein-protein interfaces. J. Mol. Biol. *318*, 161–177.

Song, L., and Rape, M. (2010). Regulated degradation of spindle assembly factors by the anaphase-promoting complex. Mol. Cell *38*, 369–382.

VanDemark, A.P., Hofmann, R.M., Tsui, C., Pickart, C.M., and Wolberger, C. (2001). Molecular insights into polyubiquitin chain assembly: crystal structure of the Mms2/Ubc13 heterodimer. Cell *105*, 711–720.

Wagner, K.W., Sapinoso, L.M., El-Rifai, W., Frierson, H.F., Butz, N., Mestan, J., Hofmann, F., Deveraux, Q.L., and Hampton, G.M. (2004). Overexpression, genomic amplification and therapeutic potential of inhibiting the UbcH10 ubiquitin conjugase in human carcinomas of diverse anatomic origin. Oncogene *3*, 6621–6629.

Williamson, A., Wickliffe, K.E., Mellone, B.G., Song, L., Karpen, G.H., and Rape, M. (2009). Identification of a physiological E2 module for the human anaphase-promoting complex. Proc. Natl. Acad. Sci. USA *106*, 18213–18218.

Wu, T., Merbl, Y., Huo, Y., Gallop, J.L., Tzur, A., and Kirschner, M.W. (2010). UBE2S drives elongation of K11-linked ubiquitin chains by the anaphase-promoting complex. Proc. Natl. Acad. Sci. USA *107*, 1355–1360.

Xu, P., Duong, D.M., Seyfried, N.T., Cheng, D., Xie, Y., Robert, J., Rush, J., Hochstrasser, M., Finley, D., and Peng, J. (2009). Quantitative proteomics reveals the function of unconventional ubiquitin chains in proteasomal degradation. Cell *137*, 133–145.

Ye, Y., and Rape, M. (2009). Building ubiquitin chains: E2 enzymes at work. Nat. Rev. Mol. Cell Biol. *10*, 755–764.

Yunus, A.A., and Lima, C.D. (2006). Lysine activation and functional analysis of E2-mediated conjugation in the SUMO pathway. Nat. Struct. Mol. Biol. *13*, 491–499.